5. Reflections on the Origin of the Broken-Egg Chaotic Attractor

Yoshisuke Ueda
Kyoto University

Abstract

We return to the context of nonlinear oscillation theory in which we began, in 1961, our experience with chaotic behavior. This context involves the systems of forced self-oscillators arising in electronic circuits. In this paper we combine earlier examples into a single mixed system, transform into a form suitable for perturbation analysis, and obtain information on the bifurcation diagram of this system. In particular, the parameter regime of the broken-egg chaotic attractor, which we discovered in analog simulation in November 1961, is mapped.

Introduction

We consider the classical context of nonlinear oscillation theory: a periodic signal is applied to a self-oscillator. The behavior of this forced system depends on the amplitude of the forcing signal, and its frequency relative to the frequency of the unforced self-oscillator. In case the forcing frequency is sufficiently close to the natural frequency of the unforced self-oscillator, and with moderate amplitude, we observe synchronous behavior: the forced system oscillates with the forcing frequency. With greater difference between the forcing and the free frequencies, we may find harmonic

oscillations (subharmonics, superharmonics, or m/n harmonics), almost-periodic motions, or even chaotic behavior.

Beginning in 1959, we were studying particular systems of this type arising in electronic circuits with triode vacuum tubes. Generalizations or combinations of the Rayleigh, Duffing, and Van der Pol systems were extensively studied, using early analog computers made in our laboratory. And in 1961, in this context, we discovered a chaotic attractor, the broken-egg attractor, which has since been found to be characteristic of many systems [1,2].

In this paper we revisit this context, with the power of modern digital computers, and some new analytical ideas, to obtain further insight into the bifurcation diagram, in which parameter regimes of the m/n harmonics and broken-egg chaotic attractor may be clearly visualized. In particular, we use the methods of perturbation theory as an analytical aid to the extensive simulations and their interpretation. The equations reduce, when damping is reduced to zero, to a particular conservative system we call the generating system.

The broken-egg chaotic attractors

We begin now with the specification of two different examples of the type of systems described above, in both of which, broken-egg attractors are observed.

Duffing/Van der Pol mixed type equation

Consider the equation

$$\frac{d^2v}{dt^2} - \mu\left(1-\gamma v^2\right)\frac{dv}{dt} + v^3 = B\cos\nu t \qquad (1)$$

This is a combination of Duffing forced pendulum and Van der Pol self-oscillator systems [1,3]. Extensive simulations of this mixed system, led to the discovery of the broken-egg attractor shown in Fig. 1 on November 27, 1961, with parameter values $\mu = 0.2$, $\gamma = 8$, $B = 0.35$ and $\nu = 1.02$.

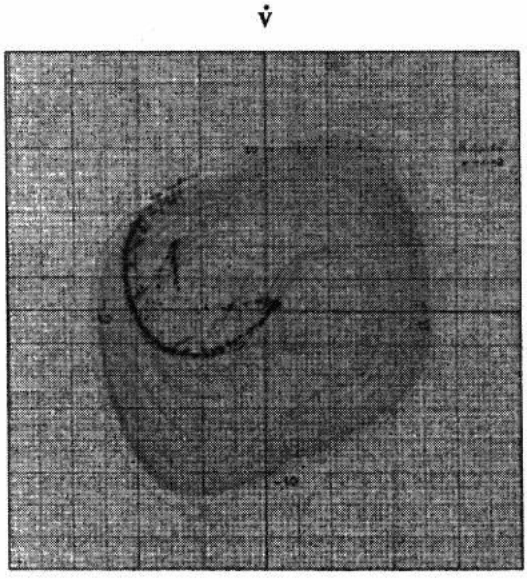

Fig. 1. Output of an analog simulation of Equation (1) with μ = 0.2, γ = 8, and B = 0.35, obtained on 27 November 1961. A continuous orbit is drawn lightly on the $v\dot{v}$ plane and points in the Poincaré section at phase zero are indicated by heavy dots. Five dots near the top are fixed points for a sequence of values at V = 1.01, 1.012, 1.014, 1.016, and 1.018. The remaining points are on the chaotic attractor with V = 1.02.

Rayleigh/Duffing mixed type equation

Consider next the equation

$$\frac{d^2v}{dt^2} - \mu\left(1 - \gamma\left(\frac{dv}{dt}\right)^2\right)\frac{dv}{dt} + v^3 = B\cos Vt \qquad (2)$$

This is a mixture of the Rayleigh and Duffing systems. Simulations in 1963 led to the Figs. 2, 3, and 4, published in 1970, with parameter values $\mu = 0.2, \gamma = 4, B = 0.3$ and $V = 1.1$[1]. By hindsight, we recognize a chaotic attractor of the broken-egg type in the ring domain, shown hatched in Fig. 4. It is the closure of the α-branch of the directly and inversely unstable 2-periodic points marked ${}^iD_j^2$, ${}^iI_j^2$ $(i,j = 1,2)$ in Fig. 3.

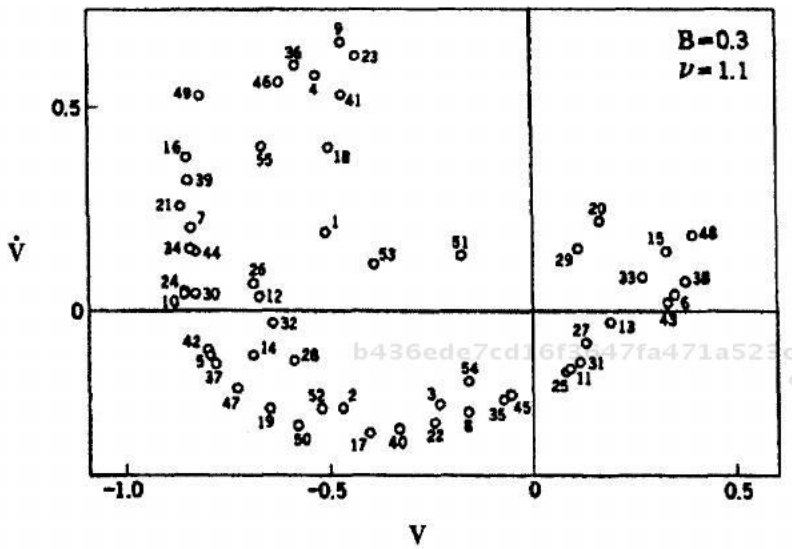

Fig. 2. Point sequence representing chaotic behavior for Equation (2) with $\mu = 0.2$, $\gamma = 4$, $B = 0.3$, and $\nu = 1.1$.

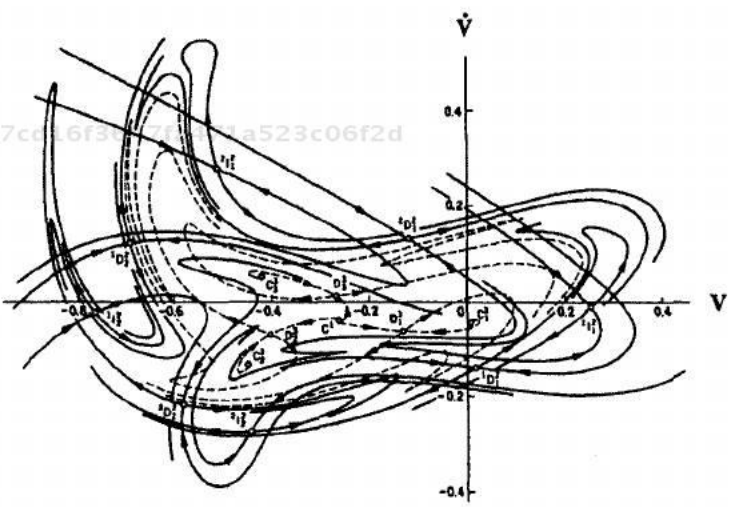

Fig. 3. Outstructure of the 2- and 3-periodic points for Equation (2) with $\mu = 0.2$, $\gamma = 4$, $B = 0.3$, and $\nu = 1.1$.

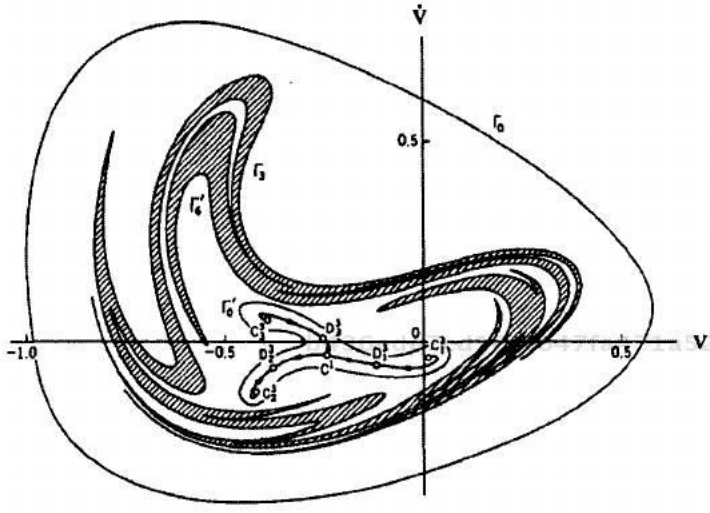

Fig. 4. Ring domain within which the chaotic broken-egg attractor for Equation (2) is confined. The parameters are $\mu = 0.2$, $\gamma = 4$, $B = 0.3$, and $\nu = 1.1$.

Parameter regimes of the broken-egg attractors

In both cases above, the broken-egg attractor is found in the regime of parameter plane of frequency and amplitude belonging to the area of the doubly periodic, or 1/2 harmonic, motion.

Modified Rayleigh/Duffing/Van der Pol equations

Next we combine the two systems discussed above into a single system. The first step is a modification of the damping term of the Van der Pol equation, introducing a fourth degree term. Then this is combined with the Rayleigh/Duffing system, resulting in these equations.

$$\begin{cases} \dfrac{du}{dt} = \mu\left(1 - u^4 - 2v^2\right)u + v \\ \dfrac{dv}{dt} = -u^3 + \mu\left(1 - u^4 - 2v^2\right)v + F\cos\nu t \end{cases} \tag{3}$$

Note that this is no longer a second order equation, due to the new term in the first equation. The parameter μ is considered a small parameter, or perturbation parameter, as we shall see below.

Without the forcing term, $F = 0$, the limit cycle representing self-oscillation is expressed by

$$u^4 + 2v^2 = 1 \tag{4}$$

Its period is given by

$$T = 4\sqrt{2}\int_0^1 \frac{1}{\sqrt{1-u^4}}du \tag{5}$$

This artificial system (3) is now the target of our analysis. We shall study the system by digital simulation to discover its qualitative phenomena.

Regimes of the various harmonic oscillations

We are now ready to present the results of the simulations of the modified system, and all of these are shown in a single map of the (v, F) parameter plane with μ fixed at 0.1, in Fig. 5.

In this map of the (v, F) parameter plane, the effects of hysteresis are suppressed. This has been done by marking only points at which a bifurcation occurs, that is an harmonic disappears, as the parameter point moves from inside to outside of a regime. Thus, what is indicated for each m/n harmonic may be regarded as the outer envelope of its regime.

Note that the regimes all have a roughly similar shape, which we call a question-mark regime. These are extensions of the tongue-shaped regimes well known in related contexts for small values of amplitude. Note also that each question-mark regime contains a shaded horned crescent-shaped regime. For example, the shaded horned crescent within the 1/2 harmonic regime is a 2/4 harmonic regime, and a parameter change from the 1/2 regime into the shaded horned crescent causes a period-doubling bifurcation. Indeed, continuing a parameter motion in this direction leads, by a period-doubling cascade, to a broken-egg chaotic attractor.

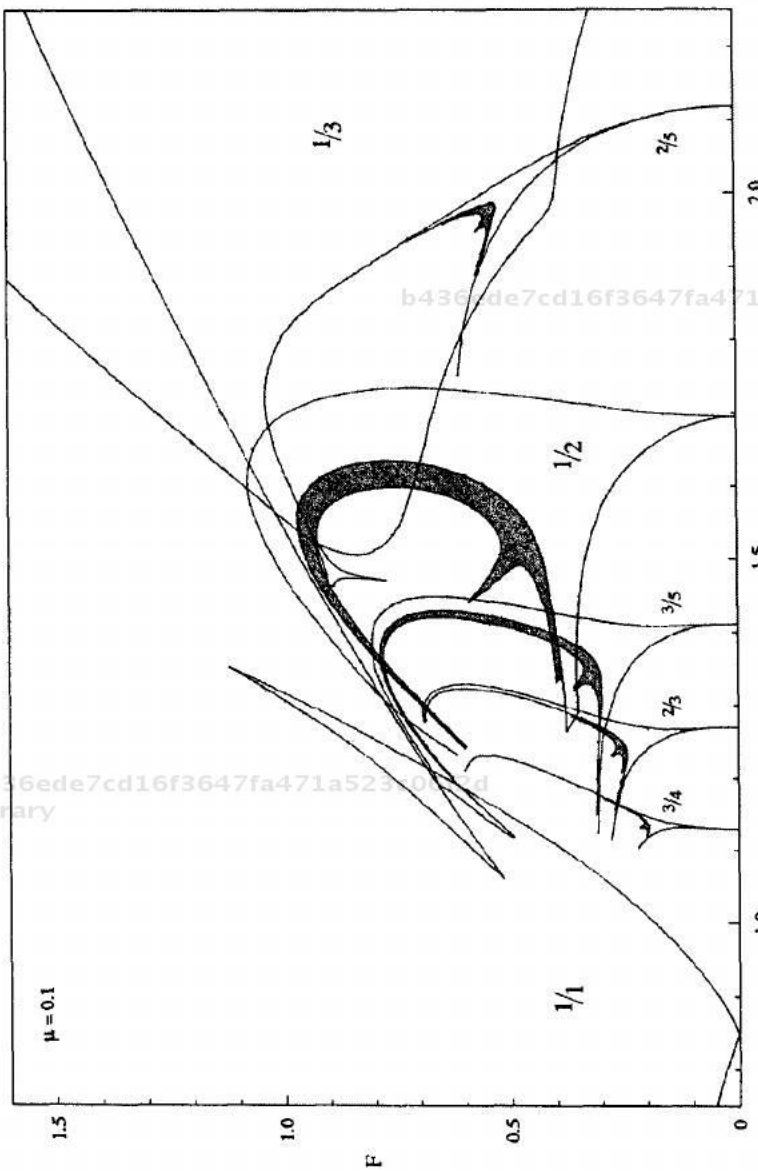

Fig. 5. Regimes of the m/n harmonic oscillations observed in the system governed by Equation (3) with μ = 0.1.

Preliminary transformation of the equation into perturbation form

Having in mind the procedures of perturbation theory, we now wish to transform our modified equation by a transformation of variables, as follows.

$$\tau = \nu t,\ x = u/\nu,\ y = v/\nu^2 \tag{6}$$

Substituting into equation (3) we obtain

$$\begin{cases} \dfrac{dx}{d\tau} = \mu\nu^3\left(\dfrac{1}{\nu^4} - x^4 - 2y^2\right)x + y \\ \dfrac{dy}{d\tau} = -x^3 + \mu\nu^3\left(\dfrac{1}{\nu^4} - x^4 - 2y^2\right)y + \dfrac{F}{\nu^3}\cos\tau \end{cases} \tag{7}$$

Proposal of a periodically forced two-dimensional system

Inspired by the new form of our system (7), we now pose a similar (but not exactly equivalent) system,

$$\begin{cases} \dfrac{dx}{dt} = \varepsilon\left(a^4 - x^4 - 2y^2\right)x + y \\ \dfrac{dy}{dt} = -x^3 + \varepsilon\left(a^4 - x^4 - 2y^2\right)y + a^3 F\cos t \end{cases} \tag{8}$$

in which the new parameter a is analogous to $1/\nu$ in (7). Note that, roughly speaking, the parameter a determines the average amplitude of the resulting oscillation. The new parameter ε is analogous to $\mu\nu^3$ of (7). However, we now regard ε as a small parameter, to be reduced gradually to zero. And in case $\varepsilon = 0$, and replacing a^3F with B, and we obtain the system,

$$\begin{cases} \dfrac{dx}{dt} = y \\ \dfrac{dy}{dt} = -x^3 + B\cos t \end{cases} \tag{9}$$

which we call the generating system.

We proposed this new system in order to simplify the analysis of equation (3). Note that equation (3) is also in perturbation form. But as the small parameter μ goes to zero, we obtain a generating system with two parameters, F and ν. But now we have a generating system with only one parameter, B.

With all this preparation, we may now present the results of our simulations of the new system (8). These are shown in Fig. 6, in which we show only three parameter regimes of the m/n harmonics, with m/n = 1/1, 1/2, and 1/3, in the parameter plane of (a,F), with $\varepsilon = 0.1$.

Within the 1/2 harmonic regime we also show, shaded, one crescent of the 2/4 harmonic.

Finally, we show as dotted curves, the loci of constant values of the new parameter, $B\left(=a^3F\right)$. On each curve, we have the same generating system.

Numerical experiments based on perturbation theory

In this section we are going to explore the behavior of the system in the perturbation form, as given in (8) above. Note in Fig. 6 that one of the contour curves of the parameter B, namely that for $B = 0.2$, is shown as a slightly heavy broken curve. We are going to explore our system along the part of this contour where the broken-egg attractor is found.

The chaotic sea within the phase portrait of the generating system

Recall that as the perturbation parameter ε decreases, we imagine the behavior of the system tending to that of the generating system, see equations (9), which is a conservative, second-order system for each value of B. But now the value of B is fixed at 0.2, and this specifies a single case of the generating system. We now consider the behavior of this particular conservative system. Figure 7 shows a "chaotic sea" in the phase portrait of this system, corresponding to a fixed phase of the forcing oscillation, as found by simulation. That is, a computed (discrete, or stroboscopic) orbit densely fills this region.

In this figure, the structure of the chaotic sea is shown as follows. First of all, the points *N, D, R* are fixed points:

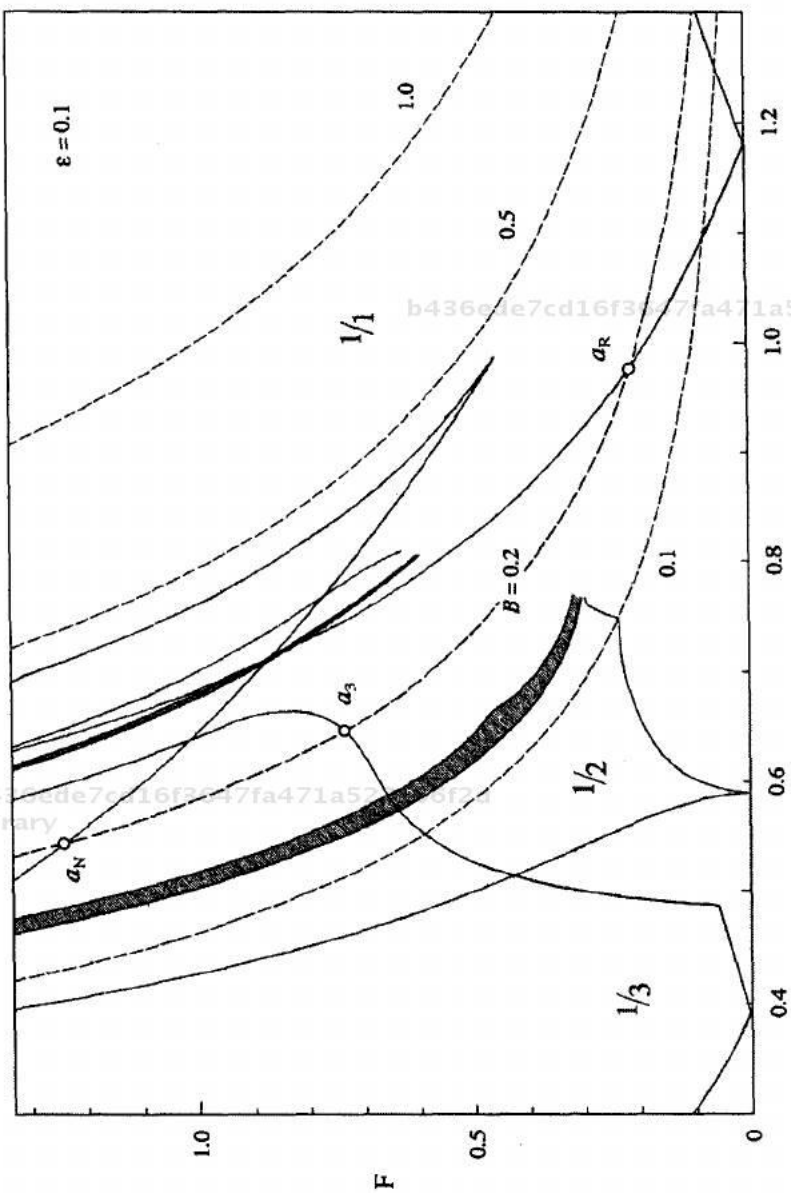

Fig. 6. Regimes of the 1/1, 1/2, and 1/3 harmonic oscillations observed in the system governed by Equation (8) with ε = 0.1.

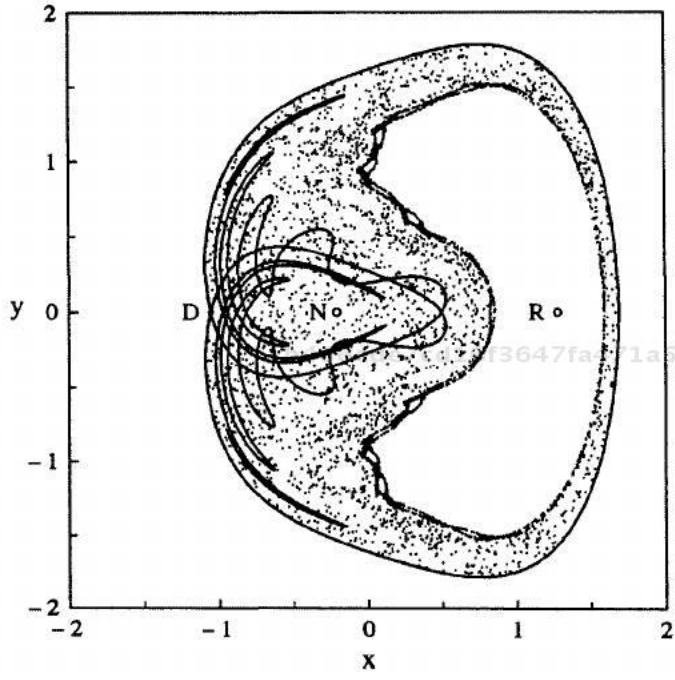

Fig. 7. Chaotic sea within the phase portrait of the generating system (9) with $B = 0.2$.

N is a stable fixed point, corresponding to a Nonresonant fundamental harmonic oscillation,
D is a Directly unstable fixed point of saddle type, and
R is a stable fixed point, corresponding to a Resonant fundamental harmonic oscillation.

Next, we see in the figure that the chaotic sea is roughly a ring domain. That is, it is topologically an anchor ring, bounded by two cycles, from which some islands have been deleted. The outer boundary, cardioid-shaped, is a nongeneric homoclinic curve. That is, the inset (ω-branch) and outset (α-branch) of the saddle point, D, coincide. The inner boundary is a necklace generated two 19-periodic orbits. One is stable center, the other is of saddle type with nongeneric homoclinic limit sets. The necklace, that is the inner boundary of the chaotic sea, is this homoclinic set.

Finally, we note the appearance of many deleted islands, in which are found stable periodic orbits. These islands are in fact organized in finite sets, which are permuted periodically by the discrete dynamics of the generating system. We have observed, in particular, some of the larger islands, having periods 1, 3, 5, 9, and so on. These aspects of the generating system are important to our study, as will appear later.

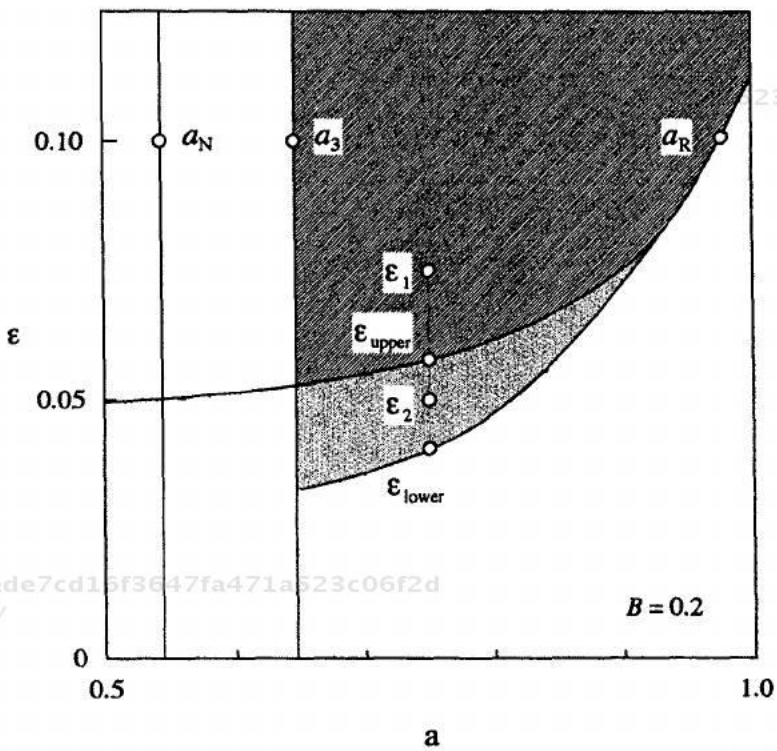

Fig. 8. Bifurcation diagram in the (a, ε) parameter plane for the Equation (8) with $B(= a^3 F) = 0.2$. Here ε plays role of perturbation parameter.

Bifurcations of the broken-egg attractor

We now consider the perturbation system as the perturbations parameter, ε, tends to zero. We will see that its portrait does not tend to that of the

generating system, but it does comes into an interesting relationship with it. We will organize our many simulations into a bifurcation diagram, showing the bifurcations of the portrait or the perturbation system, (8), as ε decreases from 0.125 to 0, for various values of a in the range 0.5 to 1.0. This bifurcation diagram is shown in Fig. 8, which we now explain.

First of all, the (a,ε) parameter regime in which the broken-egg attractor occurs is shown shaded in this figure. This is divided into two parts by a curve. In the upper part, there is a single attractor, the broken egg. And in the lower part, there coexist two attractors, the broken egg and a resonant fixed point, R, which tends to the point R described above for the generating system.

Next, consider a sequence of four points in the parameter plane of Fig. 8. These are all on the line defined by $a = 0.75$, and have ε values of $\varepsilon_1(=0.075)$, $\varepsilon_{upper}(=0.0579)$, $\varepsilon_2(=0.050)$, and $\varepsilon_{lower}(=0.0404)$. The portraits of the attractor of the perturbation system corresponding to these parameter values are given in a tableau in Fig. 9. Note that at ε_{upper}, which is on the upper bifurcation curve, the second attractor, R, appears. And at ε_{lower}, which is on the lower bifurcation curve, the broken egg vanishes in a blue sky catastrophe, and only the attractor R persists. Note that the two bifurcation curves meet at a codimension-two bifurcation point in the upper right of this diagram.

Finally, consider a sequence of points in the diagram of Fig. 8 of constant value $\varepsilon = 0.1$, but decreasing values of a, $a_3(=0.647)$, $a_N(=0.544)$. As a decreases, the broken egg vanishes by implosion to a 3-periodic point at a_3. And decreasing below a_N, there appears a nonresonant fixed point, N, corresponding to the point N discussed above for the generating system. However, when we increase a above a_3 with the same value of ε, we observe at $a_R(=0.977)$ the broken egg disappears, and only the attractor R appears.

Note. The regime of existence of the 3-periodic point attractor is shown in Fig. 6 with the label 1/3. The regimes of N and R belong to the area marked 1/1. Note that a_N, a_3, and a_R marked on this figure correspond exactly to the points labelled thus on Fig. 8. The locations of the points a_N and a_3 are nearly independent of the parameter ε, but a_R descends with decreasing ε. Thus the left-hand boundary of the 1/1 regime in Fig. 6 moves further left with decreasing ε.

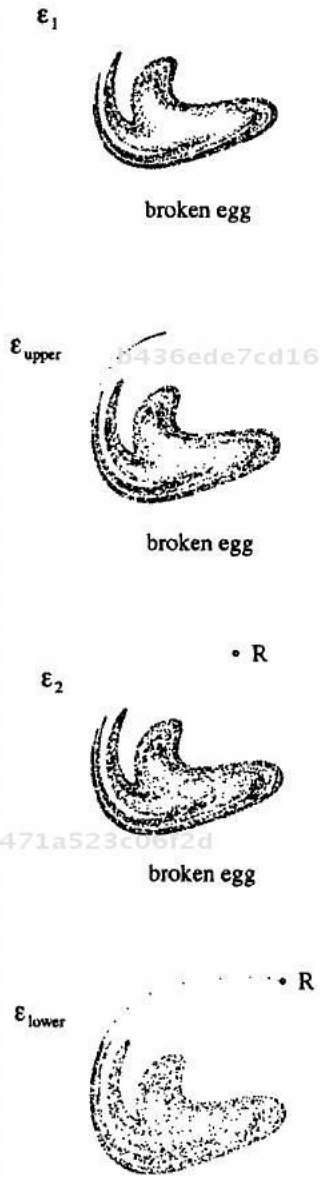

Fig. 9. Bifurcation of the broken-egg attractor and the resonant fixed point R, the parameters being $a = 0.75$ and $B\left(= a^3 F\right) = 0.2$.

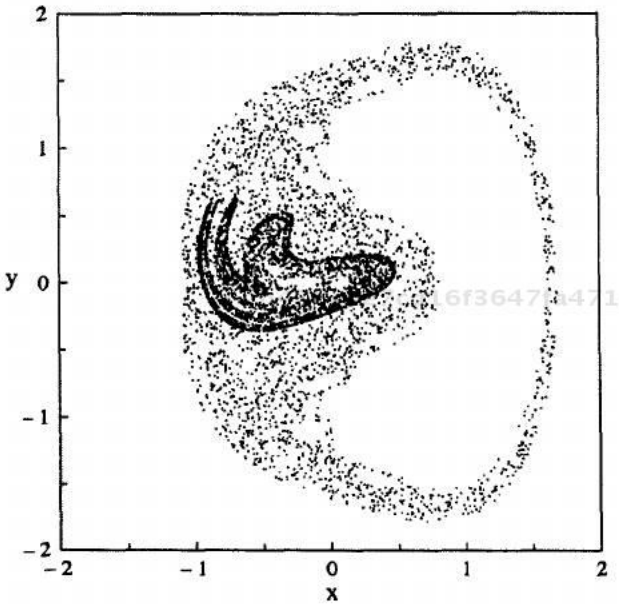

Fig. 10. The broken-egg attractor with $a = 0.75$, $a^3F(= B) = 0.2$, and $\varepsilon = 0.041$ for Equation (8) is shown inside the chaotic sea of the generating system (9) with $B = 0.2$.

Discussion

We may summarize our results in experimental perturbation theory as follows. The chaotic sea in the limit, or generating system, is the mother of the broken-egg attractor in the perturbation system, with small dissipation, ε. The discontinuous limit behavior is dissected in the bifurcation diagram, Fig. 8. A further detail regarding the approach of the baby broken egg to the mother chaotic sea is shown in Fig.10. This shows the broken egg superimposed over the chaotic sea, just before the disappearance, with $a = 0.75$, and $\varepsilon = 0.041$.

Conclusion

We now step back and regard what we have done. We began with a mixed system evolved from our earliest work in nonlinear dynamics. But we ended up with an exercise in experimental perturbation theory. We have exploring here an example in a classical theme, the near-Hamiltonian system. Experimental results such as these might well lead the way to further theoretical developments. One further direction, for example, might be a qualitative theory of perturbation for a nonlinear dynamical system. Another direction might be the inverse problem, to construct a dynamical system in analytical form corresponding to a given chaotic attractor, perhaps determined from data.

Acknowledgments

We are very grateful to Dr. Hirofumi Ohta for assistance with computer programming, Associate Professor Takashi Hikihara for various advices and Professor Ralph Abraham for discussions.

References

[1] Y. Ueda, *The Road to Chaos* (Aerial Press, Santa Cruz, CA 95061, 1992).
[2] Y. Ueda, Strange Attractors and the Origin of Chaos, in J. A. Yorke and C. Grebogi, Eds. *The Impact of Chaos on Science and Society* (United Nations University Press, 1997), pp. 324-354, Proc. Int. Symp. on The Impact of Chaos on Science and Society, Tokyo, Apr. 15-17, 1991. Also published in *Nonlinear Science Today,* Vol. 2, No. 2, pp. 1-16, Springer-Verlag, 1992.
[3] C. Hayashi, *Forced Oscillations in Nonlinear Systems* (Nippon Printing and Publishing Co., Osaka, Japan, 1953).